Valley Degeneracy in (110) Si Quantum Wells Strain and Misorientation Effects

Zhengping B. Jiang*[1], Neerav Kharche*[1,2], Gerhard Klimeck[1]

[1]Network for Computational Nanotechnology
Birck Nanotechnology Center, Purdue University
West Lafayette, IN 47907, USA
e-mail: jiang32@purdue.edu

[2]Computational Center for Nanotechnology Innovations
Department of Physics, Applied Physics, and Astronomy
Rensselaer Polytechnic Institute
Troy, NY 12180, USA

Valley degeneracy in (110) Si quantum wells (QWs) is studied. Bandstructures are computed using the nearest neighbor $sp^3d^5s^*$ tight-binding model and strain relaxation is performed by a valence force field. Two degeneracy breaking mechanisms are identified: different confinement effective mass and valley-valley interaction. Strain and electric field are both found to enhance valley splitting. Surface miscuts towards [111] direction lift the 4 fold valley degeneracy of flat (110) QWs to 2 fold, which explains the experimentally observed inconsistency. Effects of surface miscut, which could only be addressed using an atomistic method, are included in the extended supercell calculation.

valley degeneracy; tight-binding; miscut; strain; valley-valley interaction

I. INTRODUCTION

Si-based devices are being pursued for quantum computing and spintronics due to their scaling potential and integrability within the present industrial nanoelectronic infrastructure. Relative energies and degeneracies of valley states are critical for device operation in these novel computing architectures and conventional MOSFET devices at nanometer scale. Bulk Si has six equivalent conduction band minima. In (110) Si quantum wells (QWs), this degeneracy is reduced to 4 fold in the effective mass approximation (EMA) [1]. However, experimental results show ground state degeneracy factors of both 2 and 4 [2-4].

Similar inconsistencies between experimentally measured and theoretically predicted valley degeneracies are observed in (100) and (111) Si QWs [4,5,6] as well. Earlier work has shown that these inconsistencies are attributed to the presence of surface miscuts and interface disorder, which can be explicitly modeled in an atomistic method [5,6].

This work employs the tight-binding method to investigate the valley degeneracy of (110) Si QWs. Two mechanisms, (i) different confinement effective mass and (ii) valley-valley interaction are identified as the main degeneracy breaking mechanisms. A surface miscut is found to explain the experimentally observed valley degeneracy factors of 2 and 4. The effects of electric field and strain, which are commonly used to engineer the valley splitting in modern devices, are also reported.

This work is supported by Army Research Office (ARO) under award number W911NF-08-1-0527 and LPS/NSA through ARO award number W911-NF-08-1-0482, and NSF PetaApps grant number OCI-0749140.

* These authors contributed equally to this work.

II. APPROACH

A. *(110) surface model*

A rectangular unit cell of a flat (011) Si QW is shown in Fig. 1(a). The in-plane dimensions of this unit cell are $a_x=a_{Si}$ along [100] and $a_y = a_{Si}/\sqrt{2}$ along [01-1] directions, where a_{Si} is lattice constant of Si [7]. The extent along the growth direction, [011], is determined by the QW thickness. The rectangular unit cell geometry simplifies the underlying mathematics and implementation of the periodic boundary conditions in the bandstructure calculation. As explained later, the surface miscut shown in Fig. 1(b) can influence the valley degeneracy and valley splitting. The surface miscut can be easily implemented by applying the shifted boundary condition to an extended rectangular supercell.

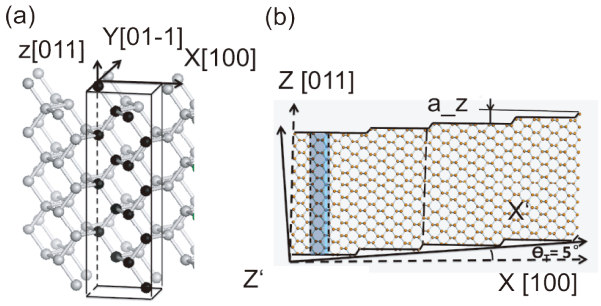

Figure 1. Atomistic schematics of unit cells. (a) Rectangular unit cell of flat QW. (b) Unit cell of a 5° miscut (110) Si QW with monolayer steps. Interface mono-atomic steps are assumed to run parallel to the (100) direction.

Here, a commonly present (011) surface miscut towards the [111] direction is studied [8,18,19]. In this configuration surface steps run perpendicular to the [100] direction. As shown in Fig. 1(b), the reduced symmetry along [100] direction results in a larger unit cell extent in that direction. The unit cell shown in Fig. 1(b) has a miscut angle of θ_T=5°. The surface normal of this QW is along [-288] direction. For an arbitrary miscut θ_T, the surface normal Z' could be [-2nn]. The miscut degree θ_T and n are related as $\theta_T = \tan^{-1}(a_z/na_x)$.

B. *Electronic structure and strain model*

The valence-force-field (VFF) method with a Keating potential is used to compute the relaxed atom positions [9, 10].

Once the atom positions are determined via VFF, the atoms are frozen in place followed by the electronic structure calculation. Strain is included in the tight-binding Hamiltonian following the prescription of [11].

Typical barrier materials like SiGe or SiO_2 will introduce biaxial strain ($\varepsilon_{//}$). This work does not include barriers directly. The effect of lattice mismatch is applied by enforcing different lattice constants in *xy*-plane according to $a_x=(1+\varepsilon_{//})a_{x0}$ and $a_y=(1+\varepsilon_{//})a_{y0}$, where a_{x0} and a_{y0} are unstrained lattice constants. Then during strain relaxation, atom positions in the whole structure and the lattice constant along *z*-direction are allowed vary to minimize strain energy.

The bandstructure is calculated using the semi-empirical nearest neighbor $sp^3d^5s^*$ tight-binding method. The dangling bonds on the QW surface are passivated. The tight-binding parameters are taken from [12, 13].

Both strain relaxation and electronic structure calculations are performed using the general purpose electronic structure simulator, NEMO-3D [9,10,14].

III. Results and Discussion

A. Valley splitting in flat QWs

The valley degeneracy in a 5nm thick flat (011) Si QW is first analyzed. In a flat (011) QW the 2 bulk valleys along [100] are projected along the same direction while remaining 4 bulk valleys are projected along [01-1] direction. The tight-binding bandstructures along [100] and [01-1] are shown in Fig. 2. The 4 valleys along [01-1] have lower energy compared to the 2 valleys along [100] direction. In the effective mass picture this splitting (Δ_{42} Fig. 2(c)) results from different confinement effective masses. The 2 valleys along [100] have lower confinement effective mass compared to the 4 valleys along [01-1], which causes Δ_{42} splitting.

The valleys along [01-1] also show a splitting (Δ_4 Fig. 2(c)), which is much smaller than Δ_{42} splitting. The valley-valley interaction causes this splitting. Similar valley-valley interaction is found in [001] Si QWs [7,15]. Such interaction cannot be modeled in a simple effective mass theory without relying on approximate perturbation theories and ad-hoc structure dependent parameters. The 4-fold degeneracy of (011) QW is reduced to 2-fold due to valley-valley interaction, which explains the reported 2-fold degeneracy for the ground state [3,4].

B. Effect of a surface miscut

Monoatomic steps (miscut) similar to those shown in Fig. 1(b) are often present at Si/SiO_2 and Si/SiGe interfaces. In Si/SiGe heterostructures miscuts are introduced intentionally to ensure uniform layer thickness. Experimentally observed 4-fold degeneracy occurs when the quantum well is formed at a miscut interface or grown on a miscut substrate.

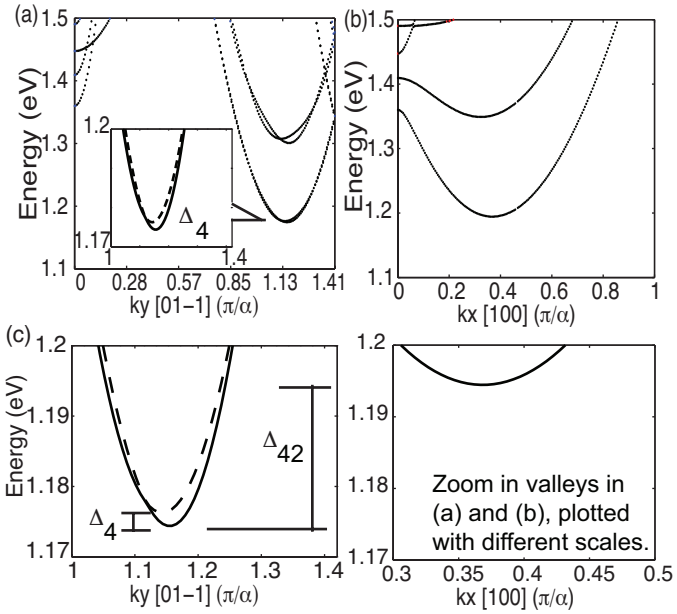

Figure 2. Bandstrcture of flat Si (110) QWs. (a) Bandstructure along symmetric direction [01-1]. Inset shows the lowest two bands and presents VS due to valley-valley interaction, which results in two pairs of valleys slightly shifted in energy. (b) Bandstructure along symmetric direction [100]. (c) Rescaling (a) and (b) to zoom in valley regions. Two figures are plotted with same energy scale to show VS due to different confinement effective masses.

To depict the geometry concept a quantum well with a 5°degree miscut towards [111] direction is shown in Fig 1(b). The extended unit cell concept of Fig. 1(b) is used to model the miscut for various different angles and the bandstructures are compared with the flat quantum well.

Fig. 3 shows 2D contour plots of lowest conduction bands of a flat and a 5° miscut (110) Si QW. Since the unit cell of a miscut QW is longer in the *x*-direction compared to unit cell of a flat QW, its Brilloin zone is shorter in the k_x-direction. Valley-valley interaction in the miscut QW is suppressed because the 4 degenerate valleys are now projected at different places in the *k*-space. As shown in Fig. 3(b) the 4 band minima are now located in four quadrants and the 4-fold degeneracy is

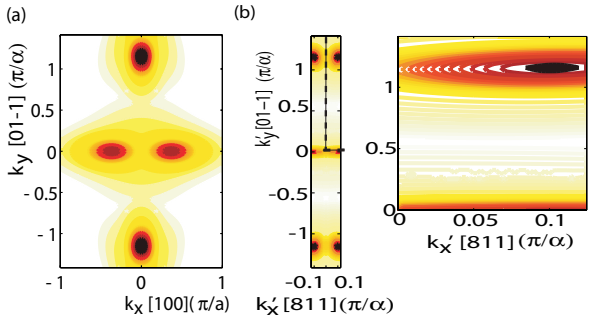

Figure 3. 2D contour plots of lowest conduction band. (a) Flat (110) Si quantum well. (b) 5° miscut (110) Si quantum well. Brillouin zone is roughly one eighth of bulk Si in kx direction due to supercell calculation. (right) Zoom in dashed area in left figure, only showing one quadrant of Brillouin zone. Positions of valley minima can be estimated by a valley projection model [16].

recovered in miscut (110) QWs [3,16]. The positions of band minima can be determined analytically by the valley projection model [16].

C. Strain and electric field

Electric fields as well as strain are known to modulate the valley splitting [7,15]. Realistic structures are subject to electric fields due to gate voltages or modulation doping and strain due to lattice mismatch at the interfaces in heterostructures such as Si/SiGe.

The valley splitting in a flat (110) Si QW as a function of the electric field and strain is shown in Fig. 4. The electric field is directed along the QW growth direction to mimic the potential well formed due to the applied gate bias in MOSFETs or the modulation doping in Si/SiGe heterostructures. To avoid the effect of truncation of the electronic domain on eigenvalues a QW thickness of 25 nm is included in the simulation domain. Due to external electrostatic potential, electrons are all pushed to gate side of QW and confined in a triangular well. In this structure, lateral confinement due to the barrier on the substrate side is quite weak and valley splitting is not sensitive to well width[15]. The QW thickness of 25 nm is sufficiently large so that the wave functions die out before reaching the barrier on substrate side for all electrical field strengths considered here. Both Δ_4 and Δ_{42} valley splittings increase monotonically with the electric field. The Δ_4 valley splitting increases [17] because the strength of valley-valley interaction increases while Δ_{24} valley splitting increases because of stronger electrostatic confinement at high electric fields. Here, the barrier layers such as SiO_2 and SiGe are not included in the electronic structure calculation. The presence of barrier typically enhances the valley splitting (Δ_4) due to the valley-valley interaction [7] and decreases valley splitting (Δ_{42}) due to the electrostatic confinement. The qualitative behavior shown in Fig.4 is however not affected by the barrier.

Strain is usually introduced by growing a QW on lattice-mismatched substrates. For example, up to 4% biaxial strain can be introduced in a Si QW grown on SiGe substrate, which has larger lattice constant than Si. Biaxial strain is found to enhance both types of valley splittings s shown in Fig. 4.

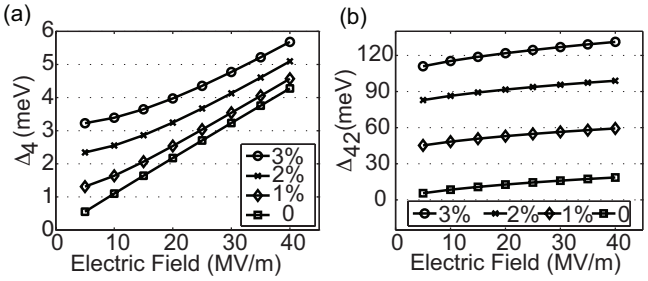

Figure 4. Effects of strain and electric field on valley splitting in 25 nm Si (110) QWs. (a) Δ_4 type valley splitting of QWs with biaxial tensile strain in the presence of electric field. 3% strain corresponds to a Ge composition of 81%. (b) Behaviors of Δ_{24} type valley splitting with same strain and electric fields in (a).

IV. CONCLUSION

In flat quantum wells, two degeneracy breaking mechanisms are identified: different confinement effective mass and valley-valley interaction. While the effective mass theory predicts a valley degeneracy factor 4 in flat well, valley-valley interaction lifts this degeneracy to 2-fold. Strain and electric field enhance both types of valley splitting. Wafer miscuts towards (111) give rise to different valley degeneracy factors from flat wells and actually results in 4-fold valley degeneracy, which explains the experimentally observed inconsistency.

ACKNOWLEDGMENT

Financial support from Army Research Office (ARO) under award number W911NF-08-1-0527 and LPS/NSA through ARO award number W911-NF-08-1-0482, and NSF PetaApps grant number OCI-0749140 is acknowledged. Computational resources of nanoHUB.org operated by the Network for Computational Nanotechnology and funded by the National Science foundation have been used for this work.

REFERENCES

[1] T. Ando, A. Fowler, and F. Stern, "Electronic properties of two-dimensional systems", Review of Modern Physics, Vol. 54, p. 437, 1982.

[2] T.Neugebauer, K. von Klitzing, G. Landwehr and G. Dorda, "Surface quantum oscillations in (110) and (111) n-type silicon inversion layers", Solid State Communication, Vol. 17, p. 295, 1975.

[3] K. C. Woo and P. J. Stiles, "Shubmikov-de Hass osillations in Si inversion layers in the (110) surface and its vicinal planes", Phys. Rev. B, Vol. 28, p. 7101, 1983.

[4] H. Kohler and M.Roos, "Valley spliting and valley degeneracy in n-type silicon (110) inversion layers", J. phys. Chem. Solids, Vol. 44, p. 579, 1983.

[5] T. B. Boykin, N. Kharche and G. klimeck, "Non-primitive rectangular cells for tight-binding electronic structure calculations", Physica E 41, p. 490, 2009.

[6] N. Kharche, S. Kim, T. B. Boykin and G. Klimeck, "Valley degeneracies in (111) silicon quantum wells", Appl. Phys. Lett. 94, 042101, 2009.

[7] N. Kharche, M. Prada, T. B. Boykin, and G. Klimeck, "Valley-splitting in strained Silicon quantum wells modeled with 2 degree miscuts, step disorder and alloy disorder", Applied Phys. Lett. 90, 092109, 2007.

[8] L.J. Sham, S. J. Allen, Jr., A. Kamgar and D. C. Tsui, "Valley valley splitting in inversion layers on a high index surface silicon", PRL, Vol. 40, No. 7, 1978.

[9] G. Klimeck, et al., "Atomistic Simulation of Realistically Sized Nanodevices Using NEMO 3-D Part I: Models and Benchmarks", Special Issue on Nanoelectronic Device Modeling in IEEE Transactions on Electron Devices, Vol. 54, p. 2079, 2007.

[10] G. Klimeck, F. Oyafuso, T. B. Boykin, R. C. Bowen, P. von Allmen, "Development of a Nanoelectronic 3-D (NEMO 3-D) Simulator for Multimillion Atom Simulations and Its Application to Alloyed Quantum Dots (INVITED)", Computer Modeling in Engineering and Science (CMES) Volume 3, No. 5 pp 601-642, 2002.

[11] T. B. Boykin, G. Klimeck, R. C. Bowen, and F. Oyafuso, "Diagonal parameter shifts due to nearest-neighbor displacements in empirical tight-binding theory", Phys. Rev. B 66, 125207, 2002.

[12] T. B. Boykin, G. Klimeck and F. Oyafuso, "Valence band effective-mass expressions in the sp3d5s* empirical tight-binding model applied to a Si and Ge parametrization", Phys. Rev. B 69, 115201, 2004.

[13] T. B. Boykin, N. Kharche and G. Klimeck, "Brillouin-zone unfolding of perfect supercells having nonequivalent primitive cells illustrated with a Si/Ge tight-binding parameterization" Phys. Rev. B 76, 035310, 2007.

[14] G. Klimeck, et al., "Atomistic Simulation of Realistically Sized Nanodevices Using NEMO 3-D Part II: Applications", Special Issue on Nanoelectronic Device Modeling in IEEE Transactions on Electron Devices Vol. 54, p. 2090, 2007.

[15] T. Boykin, et al., “Valley splitting in strained silicon quantum wells”, Applied Phys. Lett. Vol. 84, 115, 2004.

[16] F. Stern, W. E. Howard, “Properties of semiconductor surface inversion layers in the electric quantum limit”, Phys. Rev. Vol. 163, p. 816, 1967.

[17] T. B. Boykin, G. Klimeck, M. Friesen, S. N. Coppersmith, P. von Allmen, F. Oyafuso, and S. Lee "Valley splitting in low-density quantum-confined heterostructures studied using tight-binding models", Phys. Rev. B 70, 165325, 2004.

[18] K. Sata, M. Shikida, T. Yamashiro, M. Tsunekawa, S. Ito, “Roughening of single crystal silicon surface etched by KOH water solution”, Sensors and Actuators, 73, pp 122-130, 1999.

[19] K. Arima, J. Katoh and K. Endo, “Atomic scale analysis of hydrogen terminated Si(110) surfaces after wet cleaning”, APL, Vol. 85, No. 25, 2004.